Pergamon

Geochimica et Cosmochimica Acta, Vol. 58, No. 12, pp. 2725–2741, 1994

0016-7037/94 $6.00 + .00

0016-7037(94)00069-7

Olivine coronas, metamorphism, and the thermal history of the Morristown and Emery mesosiderites

ALEX RUZICKA,[1] WILLIAM V. BOYNTON,[1] and JIBAMITRA GANGULY[2]

[1]Department of Planetary Sciences, University of Arizona, Tucson, AZ 85721, USA
[2]Department of Geosciences, University of Arizona, Tucson, AZ 85721, USA

(*Received December* 16, 1992; *accepted in revised form February* 15, 1994)

Abstract—Coronas are present on all millimeter-sized mineral clasts of olivine in the Emery and Morristown mesosiderites and are a manifestation of high-temperature ($T \approx$ 850–1100°C) metamorphism. These coronas formed by reaction and diffusion between olivine and a mesosiderite-like matrix assemblage. The bulk composition of the coronas can be approximated by a mixture of ≈10–25 wt% olivine and ≈90–75 wt% metal-free matrix, except for P and Cr, which are significantly enriched in coronas. Phosphorus and Cr diffused relatively rapidly to coronas and were derived from a large volume of matrix, most likely from metal that was originally enriched in these elements prior to metamorphism. The coronas in both meteorites show a similar zone sequence, but are systematically thicker in Emery (≈800 μm wide) than in Morristown (≈350 μm wide), suggesting that Emery experienced more grain growth and more intensive metamorphism than Morristown. Textural relationships suggest that corona formation and high-temperature metamorphism occurred largely after intensive millimeter-scale brecciation and after or during metal-silicate mixing. A local equilibrium model can explain many features of the coronas, but chemical equilibrium was maintained only on a very small scale. Overgrowths are present on plagioclase in the coronas of both mesosiderites and probably formed during high-temperature metamorphism. The compositional interface between core and overgrowth plagioclase is extremely sharp, suggesting that cooling rates were ≥0.1°C/y at the peak temperature of metamorphism, consistent with high-temperature metamorphism occurring in a near-surface region of the parent body.

INTRODUCTION

MESOSIDERITES TYPICALLY consist of roughly equal amounts of Fe-Ni metal and a silicate fraction rich in orthopyroxene, plagioclase, and lesser amounts of tridymite, phosphate, and clinopyroxene (POWELL, 1969, 1971). Olivine is usually present (POWELL, 1971; FLORAN, 1978), but only in small quantities (≈2 vol% of silicates; PRINZ et al., 1980). Most mesosiderites (subgroups 1–3) are variably recrystallized, polymict impact breccias; other mesosiderites (subgroup 4) appear to be clast-laden impact melt rocks (POWELL, 1971; FLORAN, 1978; FLORAN et al., 1978; HEWINS, 1984). In the recrystallized (subgroups 1–3) mesosiderites, millimeter-sized mineral clasts of orthopyroxene, plagioclase, olivine, (inverted) pigeonite, and a variety of millimeter-sized to centimeter-sized lithic clasts (including orthopyroxenite, basalt, gabbro, and rarely dunite) are set in a matrix of finer-grained (comminuted) silicates and an interconnected network of coarse metal (POWELL, 1969, 1971; FLORAN, 1978). Thermal metamorphism resulted in coronas on olivine clasts, overgrowths of pigeonite on orthopyroxene clasts, and Mg-rich orthopyroxene rims on Fe-rich pigeonite grains, in addition to a general grain coarsening (DELANEY et al., 1981; POWELL, 1971; FLORAN, 1978; HEWINS, 1979; NEHRU et al., 1980; HEWINS, 1984). The subgroup 4 mesosiderites lack olivine coronas (FLORAN et al., 1978; HEWINS, 1984) but contain overgrowths of pigeonite on orthopyroxene (HEWINS, 1984).

Coronas in mesosiderites clearly formed by the reaction of olivine with tridymite-bearing matrix (POWELL, 1971; FLORAN, 1978; NEHRU et al., 1980). We show that a local equilibrium model for coronas can explain their mineralogical zone structure and some features of their textures and mineral compositions. Although a similar model was first proposed for the coronas by NEHRU et al. (1980), these workers concluded that "the nature of some of the [chemical] migrations that occurred are unusual and warrant further study" (p. 1117). Moreover, as coronas represent structures that have not gone to complete chemical equilibrium, they provide unique information on the reactions and diffusive processes that occurred during metamorphism, and on the nature of the original reactants prior to metamorphism. The coronas also provide constraints on the relative timing of metamorphism, metal-silicate mixing, and brecciation.

One of the most interesting aspects of mesosiderites is their cooling history. Mesosiderites appear to have cooled very slowly ($<10^{-5}$ °C/y) at low temperatures (<500°C), based on metallographic (POWELL, 1969; KULPECZ and HEWINS, 1978), fission track annealing (BULL and DURRANI, 1979; CROZAZ and TASKER, 1981), and cation ordering studies (GANGULY et al., 1994). In contrast, DELANEY et al. (1981) inferred very rapid cooling rates (up to 10–100°C/day) at high temperatures (>900°C), based on steep zoning profiles between orthopyroxene and inverted pigeonite overgrowths, but they made the incorrect assumption that the Fe-Mg diffusion coefficient in pyroxene was similar to that in olivine. Noting that Fe-Mg diffusion rates in pyroxene are likely to be a factor of $\approx 10^3$ slower than in olivine, JONES (1982) revised the cooling rates of DELANEY et al. (1981) downward to ≤2°C/y at 900–1100°C. JONES (1982) based his estimate of relative diffusion rates in olivine and pyroxene on observations of naturally zoned crystals, but did not have access to experimental diffusion data for pyroxene. The discovery of zoned plagioclase overgrowths in coronas, described here

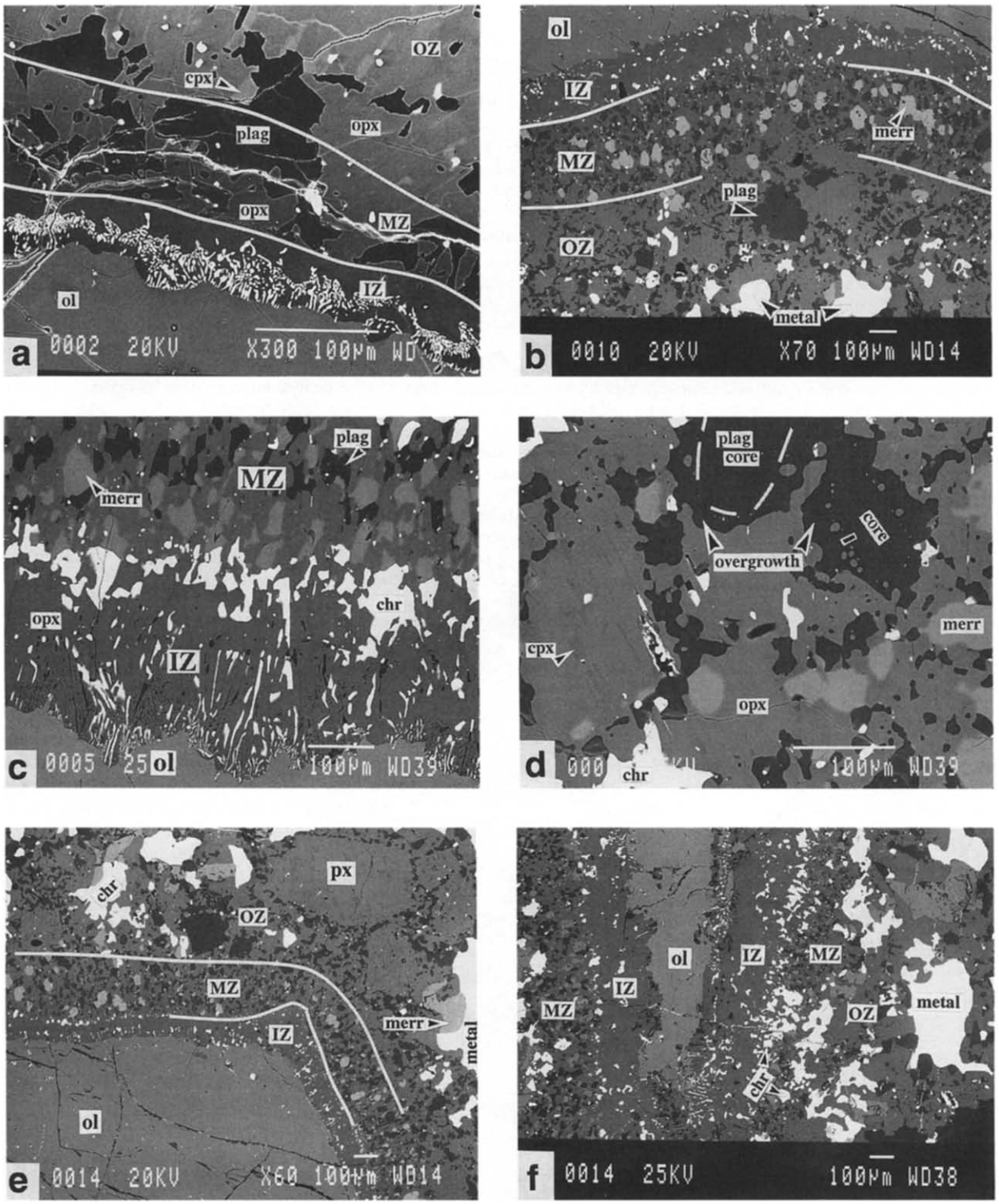

FIG. 1. Backscattered-electron (BSE) micrographs of coronas in Emery and Morristown. IZ = inner zone, MZ = middle zone, OZ = outer zone. In all figures, chromite (chr) appears white, plagioclase (plag) dark-grey or black, merrillite (merr) light-grey, and orthopyroxene (opx), clinopyroxene (cpx) and olivine (ol) various shades of medium-grey. (a) Mo-1 corona, showing subdivision of the inner zone into an outer monomineralic orthopyroxene subzone and a symplectic chromite-rich inner subzone. (b) Em-13 corona, showing the concentration of merrillite in the middle zone. (c) Close-up of the Em-1 corona, showing symplectic chromite in the inner zone, a chromite-rich band at the inner/middle zone contact, and a concentration of merrillite in the middle zone. (d) Close-up of the outer zone of the Em-1 corona, showing plagioclase overgrowths and clinopyroxene lamellae and blebs within orthopyroxene. The short dark line within the large plagioclase grain at upper right represents the location of a microprobe traverse (Fig. 6a). (e) Em-13 corona, showing a thickening of the inner zone around a corner of the olivine clast, the presence of ortho-

for the first time, allows another, more rigorous determination of the high-temperature cooling rates in mesosiderites to be made.

In this work, two mesosiderites, Emery and Morristown, were chosen for study because they contain the range of corona types previously identified by NEHRU et al. (1980) and DELANEY et al. (1981). However, both Emery and Morristown belong to the same subgroup (3A), and thus the conclusions reached in this paper may pertain to this particular subgroup only, rather than to mesosiderites in general.

METHODS

All observations were performed on two polished thin sections of Emery (AMNH 4441-2 and AMNH 4441-4) and one polished thin section of Morristown (AMNH 305-1) obtained from the American Museum of Natural History. Olivines and coronas are labelled Em (from Emery) and Mo (from Morristown). Scanning-electron-microscope (SEM) observations were carried out using an AML JEOL 840A/TN 5502 instrument at the Materials Science and Engineering Department and by a Cambridge Instruments 120B instrument at the Department of Geosciences, both at the University of Arizona. The latter instrument was used to determine modal compositions through computer-aided discrimination of phases on backscattered-electron (BSE) images. The modes have an estimated precision of $\approx$0.1–0.5 vol% for most phases. Owing to the similar atomic number of orthopyroxene and clinopyroxene in the samples, only the total abundance of "pyroxene" could be determined directly, and the proportion of clinopyroxene to orthopyroxene was estimated visually. Mineral analyses were obtained with a Cameca CAMEBAX SX-50 PGT EDS microprobe controlled by a SUN 3/360 computer at the Department of Planetary Sciences at the University of Arizona. Operating conditions were a 15 kV accelerating voltage and a 5 or 10 nA sample current for analyses of silicates, phosphate, chromite and ilmenite, and a 20 nA sample current for analyses of metal and sulfide. In all cases, a focussed beam was used. Various well-characterized mineral and glass standards were used. Analyses were generally accepted if totals ranged between 98 and 102 wt% and mineral stoichiometries were reasonable. For most oxides and elements, detection limits are estimated as <0.01 wt%, and relative analytical precision is estimated as 3–9% at a concentration of 0.5 wt%. Calculated bulk corona and matrix compositions have the following estimated relative precisions: 0.6% (SiO_2), 1–2% (MnO, CaO, Al_2O_3), 3–5% (MgO, FeO, Cr_2O_3, P_2O_5), 6–8% (TiO_2, Na_2O), and 10% (K_2O).

RESULTS

Olivine in Emery and Morristown

In Emery and Morristown, olivine occurs mainly as large (typically $\approx$1 mm across), anhedral mineral clasts, although one dunitic lithic clast was also found in Morristown. Each olivine clast has a uniform major element composition, but taken together they span a large range in composition (Fa 19–40). All are surrounded by predominantly granular- or poikiloblastic-textured coronas comprised principally of orthopyroxene and plagioclase and lesser amounts of merrillite, chromite, clinopyroxene, and ilmenite (Fig. 1). Metal is rare and tridymite is absent in the coronas, although both are present in the adjacent matrix. Olivine mineral clasts are evidently fragments of coarse-grained (>1–7 mm), olivine-rich cumulate rocks (NEHRU et al., 1980). They show uniform or slight undulose extinction indicating that they are largely undeformed or annealed. The dunite clast (Mo-5) contains olivine (91.3 vol%), orthopyroxene (7.0%), plagioclase (1.1%), chromite (0.4%), and trace metal and sulfide, with millimeter-sized, kink-banded olivine set in a seriate-textured, possibly shear-recrystallized, olivine-rich groundmass. This object was illustrated by POWELL (1971, his Fig. 19) who also commented on the severe deformation it experienced.

Corona Mineralogy and Zone Structure

Twelve olivine coronas were found in Emery, and five were found in Morristown. The coronas in Emery are large (600–1000 μm wide, average $\approx$ 800 μm) and conspicuously devoid of both coarse matrix metal and tridymite, while in Morristown, the coronas are thinner (300–400 μm wide, average $\approx$ 350 μm) and are distinguished from matrix mainly by the absence of tridymite, as the matrix adjacent to the coronas is relatively poor in metal. An important observation, whose implication is discussed later, is that the outer edge of Emery coronas is delineated by the approximately coincident disappearance of both tridymite and coarse metal; tridymite is rare on corona-facing sides of coarse matrix metal adjacent to the coronas but is often in contact with this metal on the opposite side. The coronas in both meteorites have similar, but not identical, zone structures and modal compositions (Figs. 1, 2, Table 1). In both meteorites, the coronas can be subdivided into three mineralogically distinct zones—an inner zone adjacent to olivine, rich in orthopyroxene and chromite; a middle zone, rich in orthopyroxene, plagioclase, and often merrillite; and an outer zone similar to the middle zone but containing clinopyroxene and less merrillite (Figs. 1, 2). In Morristown the inner zone can be subdivided into an orthopyroxene "subzone" that is adjacent to the middle zone, and into an orthopyroxene + chromite "subzone" adjacent to olivine (Figs. 1a, 2). The coronas in Emery are richer in merrillite and opaque minerals (chromite, ilmenite, metal, sulfide) than their counterparts in Morristown, a difference that is mirrored by the matrix in these meteorites (Table 1). The systematically thicker coronas in Emery compared to Morristown, and the otherwise similar zone sequences, suggests that Emery experienced more grain growth and more intensive metamorphism than Morristown, even though both meteorites belong to the same subgroup (3A).

NEHRU et al. (1980) originally classified coronas into three stages, based primarily on (1) the texture of the inner zone and (2) the change in Fe-Mg composition of orthopyroxene between the inner and outer zones, which is a measure of disequilibrium. DELANEY et al. (1981) expanded on this classification, proposing additional criteria based on the distribution and overall abundance of merrillite. An implication of these studies is that corona structure and texture were strongly influenced by Fe-Mg disequilibrium between olivine

pyroxene + clinopyroxene (px) clasts in the outer zone, and coarse merrillite adjacent to matrix metal. (f) Em-7 corona, showing chromite necklaces at zone contacts and a highly asymmetric distribution of chromite around olivine, with chromite being less abundant on the side of olivine facing toward a large pyroxene-rich clast (side B, left) than on the side facing a more normal metal-bearing matrix (side A, right).

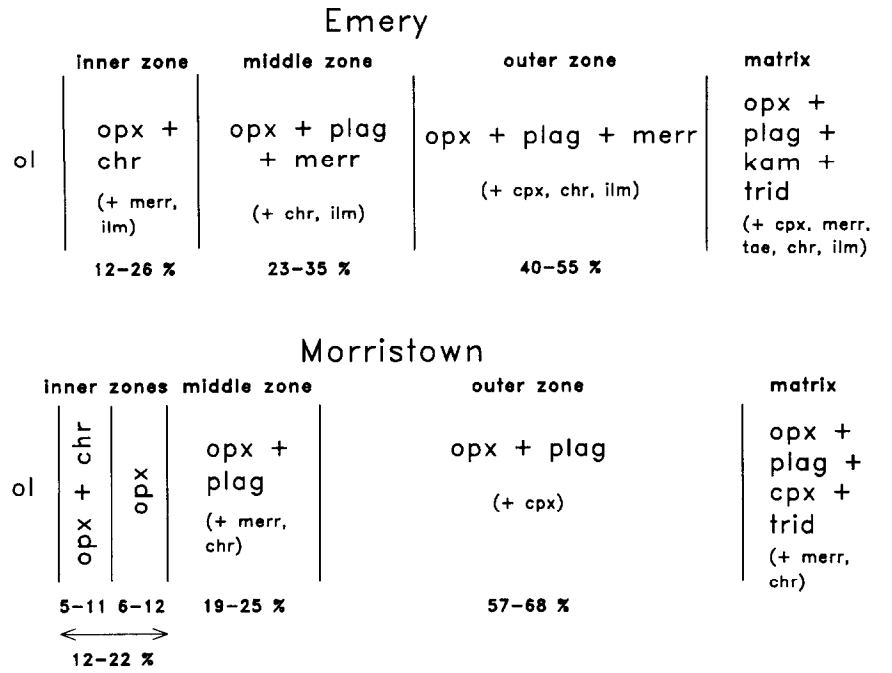

FIG. 2. Schematic zone structure of coronas in Emery and Morristown. Numbers below zones refer to fractional widths (in percent total corona thickness) of the zones. Within each zone, minerals are shown in approximate order of abundance. Opx = orthopyroxene; plag = plagioclase; merr = merrillite; chr = chromite; cpx = clinopyroxene; ilm = ilmenite; kam = kamacite; tae = taenite or tetrataenite; ol = olivine; trid = tridymite.

and matrix orthopyroxene (NEHRU et al., 1980; DELANEY et al., 1981), but based on our observations this does not appear to have been the case. All coronas have similar zone sequences (Fig. 2), and this is unrelated to Fe-Mg disequilibrium and texture. Merrillite is always concentrated in the middle corona zone (Table 1), and the texture of the inner zone appears to depend mainly on the local abundance of chromite rather than on Fe-Mg disequilibrium in the coronas. The inner zone has a symplectic texture wherever the abundance of chromite is high (Fig. 1a,c) and has a more granular texture wherever the abundance is lower.

One aspect of the coronas, relative zone widths, appears to be related to olivine composition. The outer zones of coronas are relatively thicker, and the inner zones relatively thinner, around more magnesian olivine clasts (Mo-1, Em-13) than around more ferrous olivine clasts (Table 2). Evidently, coronas that formed around forsteritic olivine experienced slightly diminished growth rates of the inner zone and slightly enhanced growth rates of the outer zone compared to other coronas. As will be shown later, this difference is consistent with a local equilibrium model for corona formation.

The identification of the original contact in coronas is useful for mass-transfer modelling. It appears that the original contact in Emery and Morristown coronas was located close to, but not necessarily coincident with, the inner/middle zone contact (cf. NEHRU et al., 1980). The inner zone is wider and the middle and outer zones are thinner where the olivine is strongly convex, such as at the ends or corners of elongate olivine grains (Fig. 1e). This pattern suggests inward-directed growth of the inner zone, and outward-directed growth of the other two zones. Moreover, the contact between the inner and middle zones is always sharp (Fig. 1c), while the contact between the middle and outer zones is more gradational. Finally, the outer zone occasionally contains small lithic clasts (Fig. 1e), and both the middle and outer zones contain likely mineral clasts of plagioclase and orthopyroxene, which implies that these two zones once comprised matrix.

Chromite in Emery coronas is concentrated in the inner zone and also sometimes forms chromite-rich bands at the inner/middle and middle/outer zone contacts (Fig. 1c, f). These chromite-rich bands ("necklaces") never make complete circuits of the olivine and may be absent altogether. Chromite is also often present as larger isolated grains within the outer zone of Emery coronas (Fig. 1e). The abundance of chromite in coronas from both Morristown and Emery is highly variable, even around individual olivine clasts, and appears to be correlated with the abundance of metal in nearby matrix. For example, chromite is much more abundant on the side of Em-7 adjacent to metal-bearing matrix than on the opposite side which is adjacent to a large orthopyroxene-rich clast (Fig. 1f). Similarly, chromite is more abundant in the inner zone of Mo-1 on the side that faces more metal-rich matrix. In the corona surrounding Em-13, chromite is less abundant in locations where large orthopyroxene and plagioclase mineral clasts in the matrix abut against the corona than in locations where coarse matrix metal is adjacent to the coronas. These observations suggest that chromite formation in the coronas of both meteorites was enhanced by the presence of nearby metal in the matrix.

Five of the twelve coronas in Emery have a core of orthopyroxene + chromite instead of olivine and are interpreted to be pseudomorphs after olivine, where the supply of olivine was exhausted by reaction, or coronas sectioned obliquely so

Table 1a. Typical modal abundances (vol %) of bulk coronas, corona zones and matrix in Emery.

phase	bulk corona	inner zone	middle zone	outer zone	matrix
orthopyroxene	57-67	80-90	60	50-60	25-30
clinopyroxene	0.5-3.5	< 0.5	< 0.1	< 5	< 5
plagioclase	16-23	< 1	20-25	20-30	20
merrillite	8-12	2-6	12-18	7-11	2-3
chromite	2-5	6-15	1-3	≤ 2	≤ 2
ilmenite	0.5-2	1-2	1	≤ 2	≤ 2
troilite	≤ 0.6	< 0.5	≤ 0.2	≤ 1	≤ 2
kamacite	≤ 1	0	≤ 0.1	≤ 2	30-35
taenite	≤ 1	≤ 0.2	0.1	≤ 2	5
tridymite	0	0	0	0	≤ 5

Table 1b. Typical modal abundances (vol %) of bulk coronas, corona zones and matrix in Morristown. Data for the inner zone refers to a bulk value including the orthopyroxene + chromite and orthopyroxene subzones.

phase	bulk corona	inner zone	middle zone	outer zone	matrix
orthopyroxene	65-75	86-92	50-65	65-75	60
clinopyroxene	0.9-4.1	< 0.1	< 0.1	≤ 5	5
plagioclase	20-28	≤ 0.2	30-45	20-30	25-30
merrillite	0.3-1.3	< 2	≤ 3	≤ 1	1
chromite	1.2-2.4	6-12	≤ 2	≤ 0.5	1
ilmenite	≤ 0.2	≤ 1	≤ 0.1	≤ 0.1	< 1
troilite	≤ 0.1	≤ 0.1	≤ 0.1	≤ 0.1	≤ 0.1
kamacite	≤ 0.1	0	0	≤ 0.1	≤ 0.1
taenite	≤ 0.1	0	≤ 0.1	≤ 0.1	≤ 0.1
tridymite	0	0	0	0	5

that the olivine was above or below the plane of the thin section. FLORAN (1978, p. 1062) provides an illustration of one of these objects.

Mineral and Bulk Compositions of Coronas

Corona orthopyroxene ranges from $En_{82}Wo_{1.2}$ (in the inner zone of Mo-1) to $En_{63}Wo_{3.8}$ (in the corona surrounding Em-2). As noted by NEHRU et al. (1980), these pyroxene compositions were strongly influenced by the composition of coexisting olivine (Fig. 3). Orthopyroxene immediately adjacent to olivine in Mo-1, Em-13, and Mo-5 is relatively magnesian and appears to be in Fe-Mg equilibrium with the olivine, while orthopyroxene at progressively greater distances from these olivine grains is more ferrous and approaches the composition of orthopyroxene in the matrix (Fig. 3). The observed Fe/Mn partition coefficient between olivine and inner zone orthopyroxene ($K_D^{Fe/Mn\ ol/opx}$) ranges from ≈ 1.3–1.8, which is similar to the value determined for equilibrium between olivine and pigeonite at magmatic temperatures ($K_D^{Fe/Mn\ ol/pig} = 1.4 \pm 0.2$; STOLPER, 1977). These data suggest that Fe-Mg-Mn local equilibrium was attained in corona pyroxene.

The compositions of corona plagioclase ($An_{87-96}Or_{<0.3}$) and merrillite are similar in Morristown and Emery and are typical for mesosiderites in general (POWELL, 1971; NEHRU et al., 1980; DELANEY et al., 1981). The composition of merrillite is uniform while that of plagioclase is more varied. Although plagioclase compositions scatter considerably, especially in Morristown, they are generally more calcic in the middle than in the outer zones (Fig. 4). Rare plagioclase grains in the inner zone of coronas have a lower An content than plagioclase at the inner/middle zone contact, suggesting that An content reaches a maximum value at the inner/middle zone contact. Some of the larger plagioclase grains near the corona/matrix contact are also appreciably zoned (see "Plagioclase overgrowths and cooling rates", below).

Microprobe analyses of chromite in Morristown were not attempted because of the fine grain size, but in Emery, chromite in the coronas and in matrix has a roughly uniform

Table 2. Differences in the relative zone widths of those coronas surrounding magnesian olivine clasts (Mo-1, Em-13) and those surrounding ferrous olivine clasts (Em-1, Em-7, Em-12, Em-18, Mo-2, Mo-3, Mo-4). Zone widths pertain to flat portions of the coronas and are expressed in terms of percent width of total corona thickness.

	Mo-1 (Fa_{19})	Em-13 (Fa_{28})	other objects (Fa_{37-40})
inner zone	12	12	16-26
middle zone	19-25	33	20-35
outer zone	63-68	55	39-55

molar Cr/[Cr + Al] ratio of ≈0.75–0.85. Chromite in the inner zones of coronas shows a tendency to be significantly enriched in Ti (X_{Ti} = molar 2Ti/[Cr + Al + 2Ti] up to 0.25) in the inner zone compared to chromite elsewhere (X_{Ti} ≈ 0.05–0.10).

A small amount (<2 vol%) of metal is present in the coronas as tiny blebs or as larger grains in contact with chromite. Most of the metal in coronas is tetrataenite (≈50 wt% Ni), in contrast to the kamacite (≈6 wt% Ni) that is prevalent as coarse grains in the matrix.

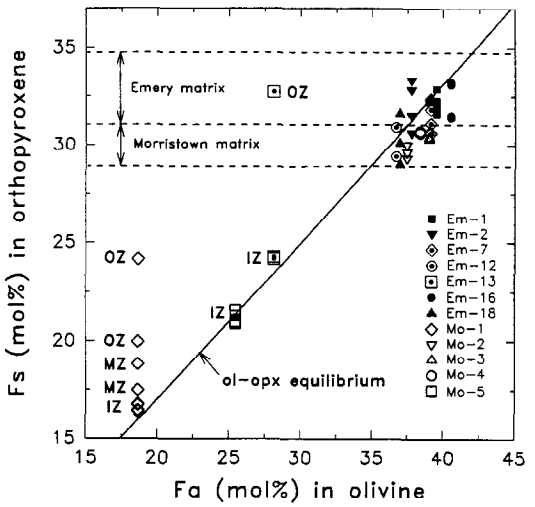

FIG. 3. Relationship between mean olivine fayalite (Fa) content and representative ferrosilite (Fs) contents in associated orthopyroxene from various corona zones (IZ = inner zone; MZ = middle zone; OZ = outer zone). Typical ranges in Fs content for matrix orthopyroxene in Emery and Morristown are also indicated. The curve labelled "ol-opx" equilibrium is based on data from MEDARIS (1969) for equilibrium pairs of olivine and orthopyroxene (T = 900°C), and is plotted by making the assumption that Fe/(Fe + Mg + Ca) ≈ Fe/(Fe + Mg) for orthopyroxene. In all cases, orthopyroxene from the inner zone of coronas closely approaches the composition expected for equilibrium with adjacent olivine.

Mineral compositions and modal data for individual corona zones were combined to determine the zone and bulk corona compositions for three representative coronas, Em-1 and Em-7 in Emery, and Mo-1 in Morristown (Table 3). (In Table 3, the average chromite composition for Emery was assumed for Morristown.) Data are presented for different sides of the olivine clasts in anticipation that corona compositions should have partially depended on the composition of the adjacent matrix. The "matrix" value for side B of the Em-7 clast (col. 8, Table 3) includes a portion of a large pyroxene-rich clast that abuts against the Em-7 corona, and thus is not representative of the overall matrix in Emery. Based on Table 3, the following observations can be made:

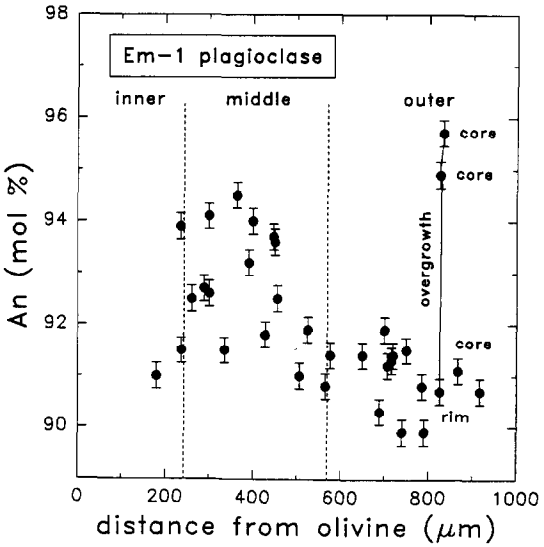

FIG. 4. Anorthite (An) content of plagioclase in a corona from Emery as a function of distance from olivine. Analyses were taken at different azimuths along a flat portion of the corona surrounding the olivine clast. The An content is generally higher in the middle zone than in the outer zone. Points labelled "core" and "rim" refer to cores and edges of overgrown grains, respectively.

Table 3. Bulk compositions (wt%) of three olivine mineral clasts (Em-1, Em-7, Mo-1), and of coronas and adjacent matrix on various sides of these clasts, in the Emery and Morristown mesosiderites. Corona and matrix compositions were reconstructed from modal and microprobe data on a metal- and sulfide-free basis, and all data were normalized to 100% prior to rounding.

	Em-1			Em-7					Mo-1				
	1	2	3	4	5	6	7	8	9	10	11	12	13
SiO_2	35.5	41.2	48.6	35.0	42.6	42.8	44.3	48.7	38.6	50.3	50.2	50.6	52.0
TiO_2	0.03	1.02	1.7	0.04	1.36	1.24	1.7	1.28	0.03	0.32	0.28	0.59	0.47
Al_2O_3	0.01	8.4	13.2	0.01	5.7	7.3	9.3	7.4	0.01	8.3	11.2	10.2	10.2
Cr_2O_3	0.03	3.4	1.2	0.01	4.5	2.7	3.4	0.88	0.03	1.27	0.82	0.86	0.61
FeO	34.2	14.9	11.7	33.69	17.6	16.0	15.0	16.6	17.9	11.8	9.1	12.5	11.8
MnO	1.33	0.88	0.65	1.33	0.95	0.85	0.78	1.02	0.52	0.51	0.43	0.55	0.58
MgO	29.2	14.6	11.4	29.4	17.2	15.7	14.0	15.7	43.8	21.4	20.1	15.2	16.0
CaO	0.03	10.1	9.3	0.02	6.7	8.9	8.3	6.4	0.03	5.36	7.0	8.1	7.6
Na_2O	0.00	0.31	0.35	0.01	0.18	0.24	0.30	0.21	0.01	0.20	0.26	0.26	0.28
K_2O	0.01	0.01	0.01	0.01	0.01	0.01	0.01	0.01	0.01	0.01	0.01	0.01	0.01
P_2O_5	0.00	5.2	1.79	0.00	3.3	4.3	3.02	1.89	0.01	0.56	0.68	1.13	0.55

1: Em-1 olivine (Fa_{40}), mean of 10 analyses.
2: Em-1 corona, side A.
3: matrix within 1-2 corona radii of Em-1, side A.
4: Em-7 olivine (Fa_{40}), mean of 15 analyses.
5: Em-7 corona, side A.
6: Em-7 corona, side B.
7: matrix within 1-2 corona radii of Em-7, side A.
8: matrix within 1 corona radii of Em-7, side B. Includes a portion of a pyroxene-rich clast adjacent to the corona.
9: Mo-1 olivine (Fa_{19}), mean of 6 analyses.
10: Mo-1 corona, side A.
11: Mo-1 corona, side B.
12: matrix within 3 corona radii of Mo-1, side A.
13: matrix within 3 corona radii of Mo-1, side B.

1) Except for Cr_2O_3 and P_2O_5, corona compositions are intermediate between that of olivine and adjacent metal-free matrix, except where large clasts abut against the corona (side B, Em-7), and except that FeO and MnO are slightly depleted relative to both olivine and matrix in the Mo-1 corona.
2) The Morristown corona has a composition more similar to that of adjacent matrix than the two Emery coronas.
3) Cr_2O_3 is consistently enriched in the coronas relative to both olivine and adjacent matrix. Relative to matrix, the coronas are enriched in Cr_2O_3 by a factor of 1.3–3.1. There appears to be a positive correlation between Cr abundance in the coronas and that in adjacent matrix.
4) The two Emery coronas are enriched in P_2O_5 relative to olivine and matrix, while this is true for only one side of the Morristown corona.

Observation 1 implies that coronas can generally be regarded as mixtures of olivine and metal-free matrix, consistent with an approximately closed-system reaction-diffusion model for the formation of the coronas. This is also illustrated by Fig. 5 for Em-1, which compares the bulk corona composition to hypothetical metal- and sulfide-free 1:3, 1:5, and 1:10 olivine:matrix (by mass) mixtures. For these mixtures, good agreement between the observed and calculated compositions is achieved for most elements, except for P and Cr, and to a lesser extent for Al and Ti. A reasonable match to the bulk corona can be generated by mixing as little as 10% or as much as 25% olivine with metal-free matrix. Mixtures richer than 25% olivine produce coronas with too much MgO and FeO, while mixtures with less than 10% olivine produce coronas with too little MgO and too much SiO_2, Al_2O_3, and TiO_2. For this corona a minimum mass discrepancy is produced for a 1:5 olivine:matrix (17% olivine) mixture.

As corona compositions can be approximated by mixtures of olivine and metal-free matrix, this suggests that matrix metal did not significantly contribute chemically to corona formation, with the possible exception of P and Cr. Evidently, most of the Fe in metal diffused away from olivine during corona formation, for otherwise the coronas would contain much more Fe^0 or FeO than they do. The same conclusion must hold for the complement of Ni in matrix metal, and for the complement of Fe and S in matrix troilite. The relatively low abundances of FeO and MnO in the Mo-1 corona suggest that FeO and MnO were partly "expelled" from the corona, probably in an attempt to maintain local equilibrium with the magnesian olivine clast (see above).

Observation 2 suggests that the ratio of olivine to matrix in the mixture that produced coronas was lower for Mo-1 than for Em-1 and Em-7. As the fractional width of the inner zone of Mo-1 ($\approx$12%) is less than that of Em-1 and Em-7 ($\approx$20–26%), this supports the conclusion, based on textural evidence (see above), that the inner zone of coronas grew in place of olivine while the middle and outer zones grew in expense of matrix. The fractional widths (volumes) of the inner zones of coronas in Emery and Morristown typically

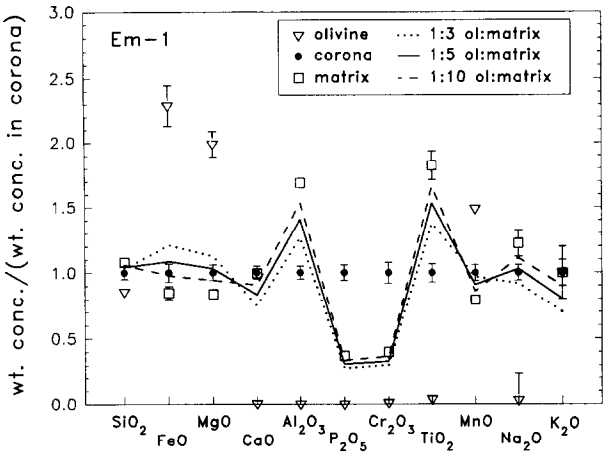

FIG. 5. Oxide concentrations in olivine, matrix, and various olivine + matrix mixtures relative to bulk corona shown on a metal- and sulfide-free basis, using data for the Em-1 corona and associated olivine and matrix. Oxides are arranged from left to right in decreasing order of abundance in the corona. Error bars represent analytical precision (errors in microprobe, modal, and zone width determinations) and are shown for data points where they exceed the size of symbols. The high concentrations of P and Cr in the corona cannot be explained by a simple mixture of olivine and matrix, but the abundances of other elements in the corona are consistent with a mixture of 10–25 wt% olivine and 90–75 wt% metal-free matrix.

range between 12–26%. Thus it appears that the coronas formed by the reaction of ≈12–26% olivine and ≈88–74% metal-free matrix.

Table 3 and Fig. 5 show that the coronas are typically enriched in both P_2O_5 and Cr_2O_3. The bulk P and Cr contents of the coronas are so high that no simple mixture of olivine and matrix, metal- and sulfide-bearing or otherwise, can account for them. It appears either that P- and Cr-rich reactants were present originally and were removed by reaction during metamorphism, or that P and Cr were transported large distances from elsewhere in the meteorite during corona formation. These topics are explored in more detail below.

Coronas: The Source of the "Excess" Phosphorus and Chromium

Our preferred interpretation is that the "excess" Cr and P in coronas was derived from a large volume of matrix metal that was initially richer in Cr and P than at present or that initially contained P- and Cr-bearing inclusions. Previous workers inferred that mesosiderite metal once contained more P, and that such metal was probably the main source of P that was ultimately used to make phosphate and schreibersite in mesosiderites (FUCHS, 1969; KULPECZ and HEWINS, 1978; CROZAZ and TASKER, 1981; HARLOW et al., 1982; CROZAZ et al., 1985). As discussed previously, the abundance of chromite in coronas correlates with the abundance of matrix metal adjacent to the coronas, which suggests that metal contributed Cr to the coronas or at least facilitated the formation of corona chromite.

The amount of matrix involved in forming corona phosphate can be estimated from the inferred initial P content of metal. HARLOW et al. (1982) determined that by putting back into metal all of the currently observed P in Emery, the initial concentration of P in metal could have been as high as 0.65 wt%. A similar calculation by KULPECZ and HEWINS (1978) suggested that Emery initially contained >0.5 wt% P in metal. The volume of matrix required to account for corona phosphate, assuming 0.65 wt% P in the metal and 40 vol% metal in matrix, is about 40–50 times the amount required to account for the coronas based on major elements. Assuming that the same volume of matrix is needed to account for corona chromite, the Cr content in, or associated with, the metal is ≈0.3 wt%.

These inferred concentrations of Cr and P are consistent with a variety of meteoritic sources of metal. Bulk compositions of iron meteorites range up to 2 wt% P and 0.25 wt% Cr (BUCHWALD, 1975), and metal grains in weakly metamorphosed ordinary chondrites contain up to ≈1 wt% each of P and Cr (RAMBALDI and WASSON, 1984; PERRON et al., 1992). Some of the P and Cr associated with ordinary chondrite metal is actually contained in tiny merrillite and chromite inclusions within the metal (PERRON et al, 1992), and most of the P and Cr in iron meteorites resides in schreibersite, chromite, and Cr-sulfide (BUCHWALD, 1975).

Chromium in the coronas may also have originated in matrix chromite that was not necessarily associated with metal. This could have occurred if the abundance of chromite in the matrix was once higher (>5 vol% in Emery and >2.5 vol% in Morristown) prior to corona formation. This is highly unlikely, however, as chromite abundances in mesosiderites (≤1.0 vol%, DELANEY et al., 1981) and in possibly related rocks such as eucrites and howardites (≤1.2 vol%, DELANEY et al., 1984) are uniformly low. Alternatively, Cr could have been derived exclusively from matrix chromite if the volume of matrix that was involved was large, comparable to the volume that supplied P to the coronas. Chromium would have to be removed not only from a large enough volume to account for the abundance of chromite in the coronas, but also to account for the abundance of chromite in the matrix adjacent to the coronas. For example, if we consider the same volume of matrix required to account for the phosphate in the coronas, then about 10% of the matrix chromite surrounding the coronas would need to be consumed. A depletion much larger than this would be clearly noticed, but none has been observed.

Thus, regardless of whether Cr originally resided in metal or chromite, it appears that Cr, like P, was extracted from a reservoir of matrix that was much larger than the reservoir that supplied other major elements to the coronas. This in turn suggests that Cr and P diffused more rapidly than other components from the matrix to the coronas. Such rapid diffusion may have occurred along (metal?) grain boundaries or possibly through metallic or silicate melt (see "Nature of metamorphism", below).

Geothermometry

The two-pyroxene geothermometer of LINDSLEY and ANDERSON (1983) was used to estimate the temperature of corona growth. The graphical geothermometer of D. H. Lindsley and coworkers allows temperatures to be determined for both clinopyroxene and orthopyroxene in each analysis pair. Analyses were obtained in the outer zone of several coronas

from each meteorite. The results show scatter, but indicate that pyroxene closure temperatures were generally higher for Emery than Morristown. This is consistent with the presence of thicker coronas in Emery than in Morristown. Based on the analysis pairs giving the most consistent results between orthopyroxene and clinopyroxene, pyroxene closure temperatures and ranges are $T = 905 \pm 25$°C for Morristown and $T = 1050 \pm 50$°C for Emery.

Plagioclase Overgrowths and Cooling Rates

Concentric overgrowths are present on the largest plagioclase grains in coronas and probably formed during high-temperature metamorphism. The interface between core and overgrowth is typically marked by a partial ring of orthopyroxene inclusions (Fig. 1d). In some cases, a sharp compositional change in FeO and anorthite content occurs across these interfaces. The cores of overgrown grains are typically lower in FeO (0.10–0.20 wt% compared to >0.20 wt%) and sometimes distinctly more anorthitic (by as much as ≈3–5 mol%) than the overgrowths and other nearby plagioclase grains. The overgrowths are most prominent in the outer zone or near the outer zone/matrix contact of coronas, although in Morristown they are also sometimes visible in the middle corona zone.

The chemical interfaces between core and overgrowth are always sharp. Microprobe traverses across two typical overgrowths suggest an apparent total diffusion length (X_A) between core and overgrowth of 3.0 ± 0.5 μm in Emery and 4.5 ± 0.5 μm in Morristown (Fig. 6). A more precise estimate for X_A can be obtained for the Morristown overgrowth by matching a best-fit, calculated diffusion profile to the observed profile assuming that diffusion occurs between two compositionally uniform halfspaces; this suggests $X_A \approx 4.4$ μm (Fig. 6b).

The sharpness of these chemical discontinuities in plagioclase constrain the thermal history of Emery and Morristown during and subsequent to corona formation. GANGULY et al. (1994) derived cooling rate expressions for "exponential" and "asymptotic" cooling models, the latter of which is assumed here. For asymptotic cooling,

$$\frac{1}{T} = \frac{1}{T_0} + \eta t, \qquad [1]$$

where T = temperature (K), T_0 = initial (maximum) temperature (K), t = time (s), and η = a cooling rate parameter ($K^{-1}\,s^{-1}$) that is independent of temperature and time once the maximum temperature is specified. For this cooling model, the cooling rate is given by

$$\frac{dT}{dt} = -\eta T^2 = \frac{-64 D(T_0) R}{Q X^2} T^2, \qquad [2]$$

where $D(T_0)$ = the diffusion coefficient at the initial temperature, Q = activation energy for diffusion, R = gas constant, and X = the total length of the diffusion zone (GANGULY et al., 1994).

Cooling rates were calculated by assuming a temperature given by the two-pyroxene method ($T = 1050 \pm 50$°C for Emery and 905 ± 25°C for Morristown) and by assuming that NaSi-CaAl interdiffusion in plagioclase occurred under "dry" conditions, with Q and $D(T_0)$ based on the work of GROVE et al. (1984). The apparent diffusion length (X_A) will be larger than the actual diffusion length (X) because of the spatial averaging intrinsic to microprobe analyses. The spatially averaged analyses were deconvolved using the method of GANGULY et al. (1988). Assuming a value of $\epsilon = 0.6$ μm in the equations of GANGULY et al. (1988), the diffusion lengths may be estimated as $X \leq 0.85$ μm for Emery (corresponding to $X_A \leq 3.5$ μm) and $X \approx 2.7$ μm for Morristown (corresponding to $X_A \approx 4.4$ μm).

Making these assumptions, the calculated initial cooling rates are ≥0.4°C/y ($T_0 = 1050$°C) or ≥2°C/y ($T_0 = 1100$°C) for Emery, and $\approx 10^{-4}$ °C/y ($T_0 = 900$°C) for Morristown. If Morristown was heated to the same temperature as Emery, then its initial cooling rate would have been ≈0.03°C/y ($T_0 = 1050$°C) or ≈0.2°C/y ($T_0 = 1100$°C). Neglecting the

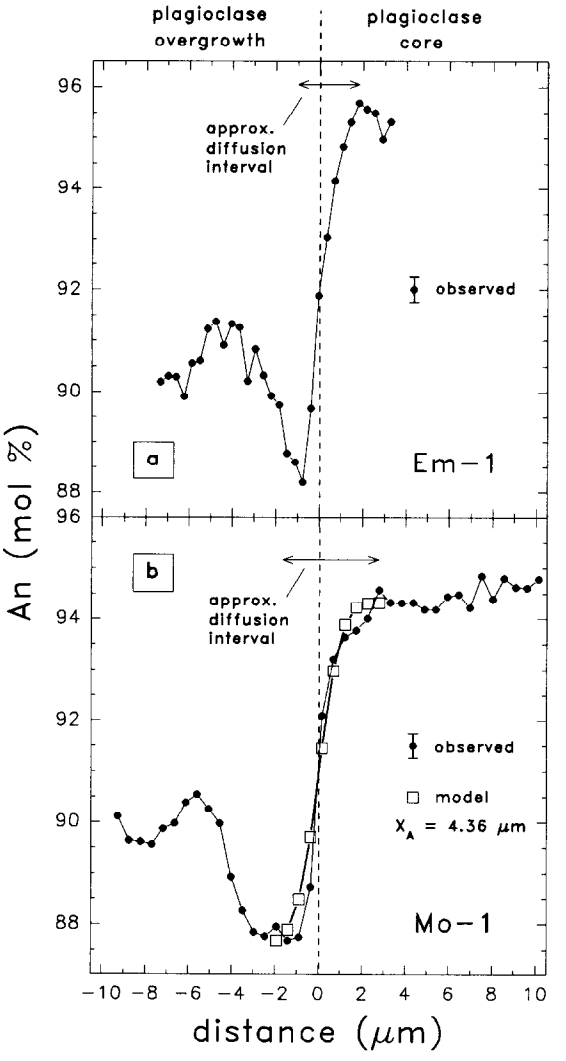

FIG. 6. Microprobe traverse data across the core-overgrowth interfaces of two plagioclase grains in Emery (a) and Morristown (b). The approximate interface boundary in both profiles is taken as the point where the concentration has changed by half of the total amount. Both profiles are asymmetric. A calculated profile (squares) in (b) assumes an initial concentration change of 6.64 An mol% and a characteristic diffusion length (X_A) of 4.36 μm.

effect of spatial averaging (i.e., using X_A instead of X in Eqn. 2) decreases the calculated cooling rates by factors of $\approx$2.5 for Morristown and 10–20 for Emery. Altogether, the data are broadly consistent with a cooling rate of $\geq$0.1°C/y at the highest metamorphic temperatures ($\approx$1100°C).

These cooling rates are similar to the cooling rates of 0.01°C/y and 0.1°C/y at 1150°C inferred for the Lowicz and Clover Springs mesosiderites, respectively, by GANGULY et al. (1994), based on zoning in orthopyroxene overgrowths and a re-evaluation of Fe-Mg diffusion kinetics in orthopyroxene. Although the calculated cooling rates vary somewhat, these apparent variations may not be significant, both because diffusion anisotropy in the minerals is not explicitly taken into account, and because small errors in temperature estimates lead to large differences in the cooling rates.

The diffusion lengths across the core-overgrowth interfaces also constrain the cooling rates of Emery and Morristown at lower temperatures. The cooling rates could not have been as low as 10^{-6} °C/y above $\approx$ 800–825°C without resulting in significant diffusion within the overgrowths, regardless of the maximum temperature during high-temperature metamorphism. This conclusion is consistent with diffusion profiles in orthopyroxene overgrowths in Lowicz and Clover Springs (GANGULY et al., 1994), and it is also consistent with the observed anisotropy in natural remanent magnetism (NRM) directions in some mesosiderites, which suggests that any late, low-temperature annealing occurred below the Curie point of metal, $\approx$700°C (RUBIN and MITTLEFEHLDT, 1993).

μ Gradients and Local Equilibrium

As shown below, a local equilibrium model can explain most of the salient features of the coronas. In this model, the mineral assemblages are considered to be in local equilibrium with an "exchange medium." The exchange medium may correspond to an intergranular fluid, a zone of crystalline disorder near grain boundaries or dislocations, or a surface film adsorbed onto crystal surfaces (e.g., JOESTEN, 1977). Reactions occurring between the exchange medium and the coexisting solids will buffer the chemical potentials (μ_i) in the exchange medium, and differences in the mineral assemblage from one zone to another will produce gradients in these potentials. As diffusion will tend to move components away from regions where these components have high μ to where these components have lower μ, an analysis of μ gradients in coronas may be used to predict the directions that components should diffuse.

Assuming constant pressure, temperature, mineral composition, and local equilibrium between the exchange medium and mineral phases, the following expression may be used to constrain μ gradients in the exchange medium (KORZHINSKII, 1959, his Eqn. 59; JOESTEN, 1977):

$$\sum_i N_i^\phi \, \partial\mu_i^{\text{e.m.}} = 0, \qquad [3a]$$

where N_i^ϕ = molar proportion of component i in mineral ϕ, and $\partial\mu_i^{\text{e.m.}}$ = change in chemical potential of component i in the exchange medium. "i" refers only to those components that are locally buffered by mineral phases and does not apply to any components that are buffered by the medium external to the local volume of interest. At constant pressure and temperature, it can also be shown that the following expression is valid for local equilibrium:

$$\sum_i N_i^\phi \, \partial\mu_i^{\text{e.m.}} = \partial\mu_j^\phi \quad (j = \sum_i N_i^\phi \, i), \qquad [3b]$$

where $\partial\mu_j^\phi$ = change in the chemical potential of component j in mineral ϕ, and "j" represents a linear combination of the "i" components.

The principal minerals within and adjacent to olivine coronas in mesosiderites are orthopyroxene, calcic plagioclase, merrillite, diopsidic clinopyroxene, chromite (a complex solid solution of Cr-spinel, Al-spinel, and Ti-spinel), olivine, and tridymite. Ilmenite is also present in small quantities throughout the coronas. Applying Eqn. 3a to each of these minerals results in the equations given in Table 4. Depending on which minerals coexist locally, one or more of the buffering relations given in Table 4 will apply to constrain the possible variations in chemical potentials. For example, the outer zones of coronas can be modelled to contain orthopyroxene, plagioclase, merrillite, and diopside, with μ variations constrained by relations [a–d] in Table 4; while the inner zone of coronas can be modelled to contain orthopyroxene, chromite and small amounts of ilmenite, with μ variations constrained by relations [a], [g–i], and possibly [j] in Table 4.

The constraints on chemical potential gradients can be visualized by using three-dimensional chemical potential saturation diagrams (Fig. 7), following KORZHINSKII (1959, pp. 90–98), JOESTEN (1977), and others. Buffering by mineral phases constrain the μ_i to lie on "saturation" or "buffering" planes or lines in chemical potential space. The absolute position (distance from origin) of the saturation planes and lines depend on temperature and pressure, but for fixed mineral compositions the slopes of the planes and lines depend only on compositions of the minerals. If μ_i lies below the saturation potential (closer to the origin) of any given phase, then this phase will be metastable for that μ_i.

Buffering by both tridymite and orthopyroxene, as in the matrix and as at the outer zone/matrix contact, requires the μ_i to be somewhere along the curved line containing point **m** in Fig. 7a, while buffering by olivine and orthopyroxene, as at the olivine/inner zone contact, requires the μ_i to be along the curve that contains points **o1**, **o2**, and **o3** in this figure. The local bulk composition determines where along these two lines the potentials actually lie. Point **o1** represents buffering by a relatively Mg-rich olivine, and point **o3** by a relatively Fe-rich olivine. Points **o1**, **o2**, and **o3** are chosen so that $\partial\mu_{FeO} \approx 0$, $\partial\mu_{FeO} \approx \partial\mu_{MgO}$, and $\partial\mu_{MgO} \approx 0$, respectively, along the dashed paths to point **m**.

Provided that the composition of the system is not too FeO-rich, Fig. 7a suggests that tridymite and olivine must be removed from the coronas, because close to olivine μ_{SiO_2} lies below the saturation surface for tridymite, and close to tridymite μ_{MgO} and μ_{FeO} lie below the saturation surface for olivine. This is consistent with the absence of olivine and tridymite within coronas.

Where the Fe/Mg ratio of orthopyroxene changes little across the coronas, as is true for most of the coronas in Emery and Morristown, the μ variations must resemble path **m-o2** (Fig. 7a), and both μ_{FeO} and μ_{MgO} increase almost equally

Table 4. Constraints on chemical potential changes in the exchange medium (e.m.) as a result of buffering by mineral phases, assuming constant pressure, temperature, and mineral compositions. w = molar Ca/(Ca+Na) in plagioclase, x = molar Fe/(Fe+Mg) in orthopyroxene, y = molar Fe/(Fe+Mg) in olivine, z = molar Fe/(Fe+Mg) and v = molar Cr/(Cr+Al) in spinel.

buffering mineral*	constraint on chemical potential change	
Opx	$(1-x)\partial\mu_{MgO}^{e.m.} + x\partial\mu_{FeO}^{e.m.} + \partial\mu_{SiO_2}^{e.m.} = 0$	[a]
Plag	$w\partial\mu_{CaO}^{e.m.} + (1-w)\partial\mu_{NaO_{1/2}}^{e.m.} + (1+w)\partial\mu_{AlO_{3/2}}^{e.m.} + (3-w)\partial\mu_{SiO_2}^{e.m.} = 0$	[b]
Merr	$3\partial\mu_{CaO}^{e.m.} + 2\partial\mu_{PO_{5/2}}^{e.m.} = 0$	[c]
Diop	$0.5\partial\mu_{CaO}^{e.m.} + 0.5\partial\mu_{MgO}^{e.m.} + \partial\mu_{SiO_2}^{e.m.} = 0$	[d]
Ol	$(2-2y)\partial\mu_{MgO}^{e.m.} + 2y\partial\mu_{FeO}^{e.m.} + \partial\mu_{SiO_2}^{e.m.} = 0$	[e]
Trid	$\partial\mu_{SiO_2}^{e.m.} = 0$	[f]
Cr-sp	$[v]\ \{(1-z)\partial\mu_{MgO}^{e.m.} + z\partial\mu_{FeO}^{e.m.} + 2\partial\mu_{CrO_{3/2}}^{e.m.}\} = 0$	[g]
Al-sp	$[1-v]\ \{(1-z)\partial\mu_{MgO}^{e.m.} + z\partial\mu_{FeO}^{e.m.} + 2\partial\mu_{AlO_{3/2}}^{e.m.}\} = 0$	[h]
Ti-sp	$(2-2z)\partial\mu_{MgO}^{e.m.} + 2z\partial\mu_{FeO}^{e.m.} + \partial\mu_{TiO_2}^{e.m.} = 0$	[i]
Ilm	$\partial\mu_{FeO}^{e.m.} + \partial\mu_{TiO_2}^{e.m.} = 0$	[j]

* Opx = orthopyroxene ($Mg_{1-x}Fe_xSiO_3$); Plag = plagioclase ($Ca_wNa_{1-w}Al_{1+w}Si_{3-w}O_8$); Merr = merrillite ($Ca_3[PO_4]_2$); Diop = diopsidic clinopyroxene ($Ca_{0.5}Mg_{0.5}SiO_3$); Ol = olivine ($Mg_{2-2y}Fe_{2y}SiO_4$); Trid = tridymite (SiO_2); Cr-sp = Cr-spinel component in chromite ($Mg_{1-z}Fe_zCr_2O_4$); Al-sp = Al-spinel component in chromite ($Mg_{1-z}Fe_zAl_2O_4$); Ti-sp = Ti-spinel component in chromite ($Mg_{2-2z}Fe_{2z}TiO_4$); Ilm = ilmenite ($FeTiO_3$)

while μ_{SiO_2} decreases from matrix to olivine. An increase in μ_{FeO} from matrix to olivine has two important implications. First, it suggests that some metal would be oxidized during corona formation, consistent with the tendency for metal in coronas to be Ni rich. Second, it suggests that most of the Fe liberated from the breakdown of matrix metal would diffuse away from olivine and not become incorporated into coronas.

The topology of Fig. 7a also provides an explanation for the difference in relative zone widths observed between coronas surrounding more magnesian olivines and those surrounding more ferrous olivines (Table 2). For a magnesian olivine grain, $\partial\mu_{MgO}$ across the coronas, and hence the flux of MgO away from olivine, will be larger than for a more ferrous olivine grain. This should allow increased production of Mg-rich phases such as orthopyroxene and clinopyroxene at greater distances from the olivine, increasing the thickness of the outer zone relative to the inner zone.

Fig. 7b suggests that $\mu_{AlO_{3/2}}$ will generally reach a maximum within the coronas and will decrease toward both olivine and matrix. This maximum occurs at a location where anorthite + spinel + enstatite coexist and together serve as buffers (point **im** in Fig. 7b), which corresponds to the inner/middle zone contact in Emery coronas.

A local maximum in $\mu_{AlO_{3/2}}$ at the inner/middle zone contact in coronas is suggested by the variation of Al content in orthopyroxene (Fig. 8). Al_2O_3 in orthopyroxene typically increases from $\approx$0.5–0.6 wt% in the matrix to a maximum of $\approx$0.9–1.4 wt% at the inner/middle zone contact before decreasing toward olivine again (Fig. 8). These trends are consistent with buffering of Al by orthopyroxene and anorthitic plagioclase in the middle and outer zones of coronas, and by orthopyroxene and a $(Mg,Fe)Al_2O_4$ component in chromite in the inner zone of coronas.

Relatively high $\mu_{AlO_{3/2}}$ within the coronas will tend to result

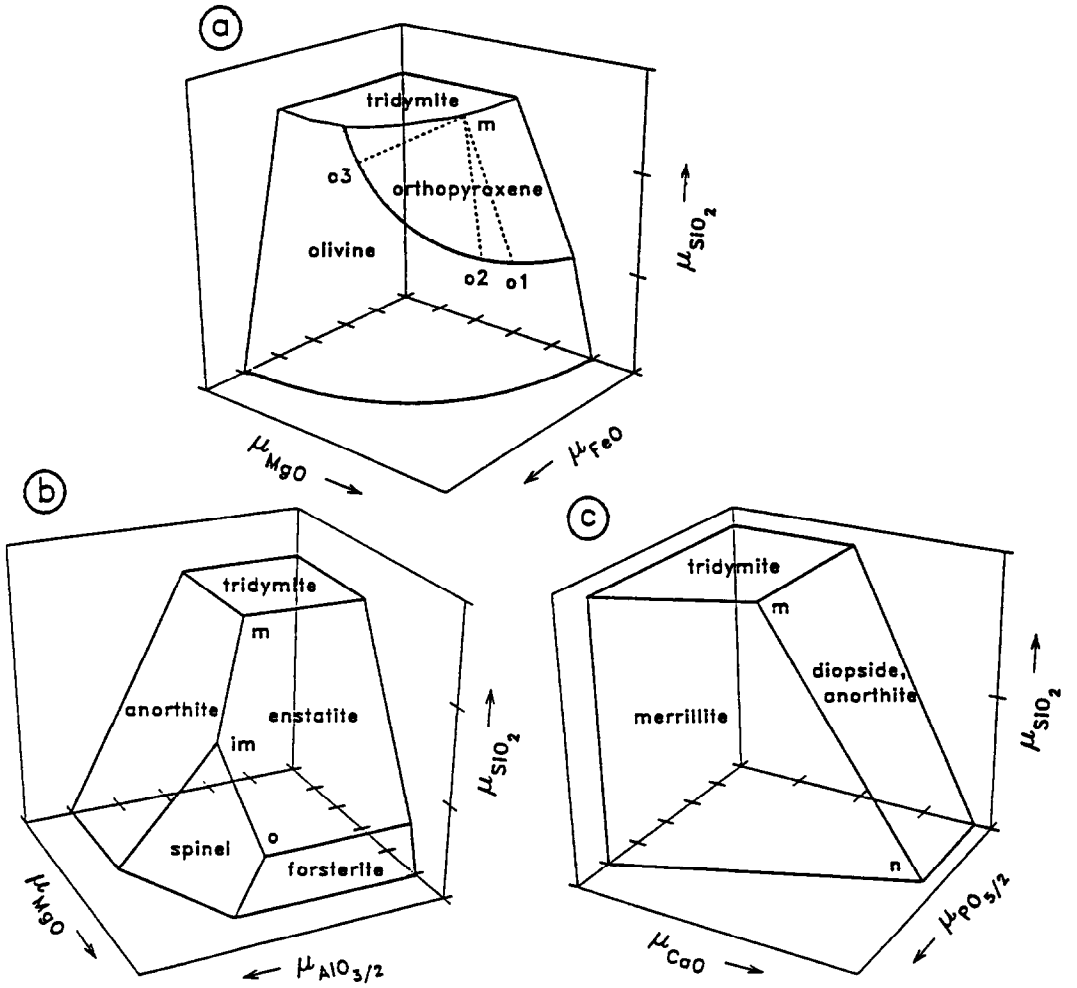

FIG. 7. Chemical potential (μ) saturation diagrams for (a) μ_{FeO}-μ_{MgO}-μ_{SiO_2}, (b) μ_{MgO}-$\mu_{AlO_{3/2}}$-μ_{SiO_2}, and (c) μ_{CaO}-$\mu_{PO_{5/2}}$-μ_{SiO_2}, showing saturation surfaces for various minerals. Point m corresponds to the corona/matrix contact in all diagrams. In (a), points o1, o2 and o3 correspond to the olivine/inner zone contact for various Fe/Mg ratios in olivine and inner zone orthopyroxene; the dashed curves show the locus of μ_i between olivine and matrix. In (b), point o corresponds to the olivine/inner zone contact and point im to the inner/middle zone contact. In (c), point n corresponds to a location somewhere within the middle or outer zones of coronas; in this diagram the diopside and anorthite saturation surfaces have the same slope and for simplicity are shown to be coincident, but in reality these surfaces generally will not coincide.

in the diffusion of $AlO_{3/2}$ towards both olivine and matrix. Under certain conditions this will result in a centrally located, Al-poor zone in coronas. Indeed, Morristown coronas contain a nearly monomineralic orthopyroxene subzone between the more Al-rich, plagioclase-bearing middle zone and the more Al-rich, chromite-bearing zone immediately adjacent to olivine (Figs. 1a, 2). Moreover, diffusive transport of $AlO_{3/2}$ toward both olivine and matrix should result in the production of Al-bearing minerals adjacent to olivine (more Al-spinel) and adjacent to matrix (more plagioclase). A plagioclase-forming reaction near the corona/matrix contact of coronas is consistent with textural evidence for the formation of plagioclase overgrowths near the corona/matrix contact and in the outer zones of coronas.

Note that if anorthite + tridymite + enstatite locally coexist in equilibrium, then Al spinel can coexist with forsterite and enstatite but not with tridymite (Fig. 7b). This suggests that a pure $(Mg,Fe)Al_2O_4$ spinel component is stable close to olivine but unstable in zones closer to matrix. The stability of Al-spinel close to olivine may be the reason why chromite is concentrated in the zone adjacent to olivine in mesosiderite coronas.

Buffering by Ca-plagioclase, merrillite, and diopside (Eqns. [b–d] in Table 4) should have controlled the variations in $\mu_{PO_{5/2}}$ and μ_{CaO} in the middle and outer zones of the coronas (Fig. 7c). Figure 7c suggests that in moving from the corona/matrix contact (point **m**) toward olivine (in the direction of point **n**), μ_{SiO_2} and $\mu_{PO_{5/2}}$ will decrease while μ_{CaO} will increase. This implies that CaO would have tended to diffuse away from olivine, while SiO_2 and $PO_{5/2}$ would have tended to diffuse toward olivine.

As merrillite is the only phase that contains significant P in coronas, diffusion of $PO_{5/2}$ toward olivine requires merrillite to be removed by reaction at the corona-matrix contact and to be produced by reaction closer to olivine. These reactions and the consequent concentration of merrillite toward

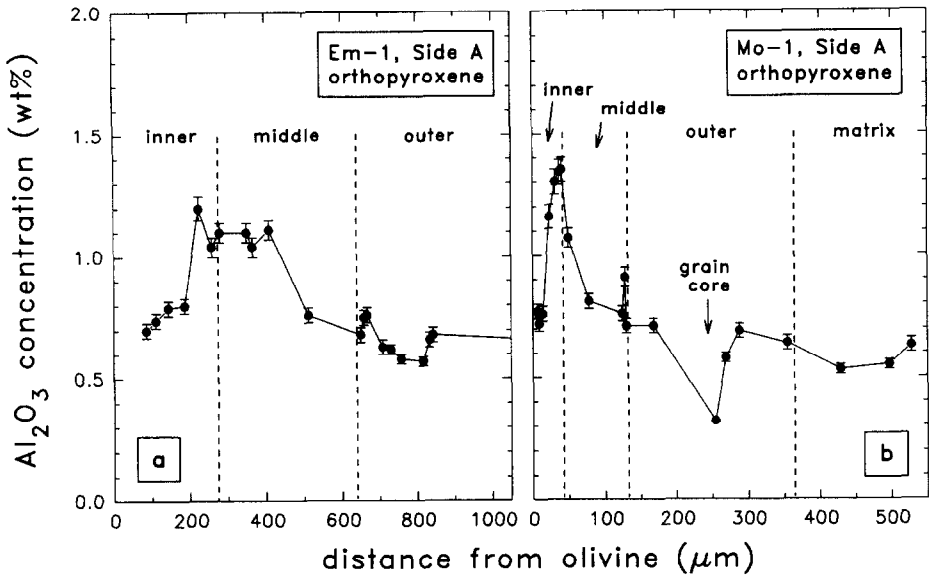

FIG. 8. Concentration of Al in orthopyroxene as a function of distance from olivine for (a) a corona from Emery and (b) a corona from Morristown. Analyses were taken at different azimuths along flat portions of the coronas surrounding the olivine clasts. One analysis of Morristown pyroxene (labelled "grain core") corresponds to the core of an especially large grain that is relatively low in Al, Cr, and Ti, and which appears to be out of equilibrium with the surrounding pyroxene.

olivine can continue so long as merrillite is locally present and able to contribute to the buffering of $PO_{5/2}$. The relatively low abundance of merrillite immediately adjacent to olivine in the inner zone is therefore consistent with this zone having grown in place of olivine, where merrillite was absent originally. Thus, the concentration of merrillite in the middle zone of coronas is readily explainable in terms of a local equilibrium model.

The systematic, corona-wide change in plagioclase composition (Fig. 4) is also consistent with local equilibrium. A small increase in the anorthite ($w = Ca/(Ca + Na)$) content of plagioclase from matrix to the inner zone implies that $\partial\mu^{plag}_{Ca_wNa_{1-w}Al_{1+w}Si_{3-w}O_8} > 0$ over this interval. The latter quantity can be expressed in terms of μ changes in the exchange medium by using Eqn. 3b:

$$\partial\mu^{plag}_{Ca_wNa_{1-w}Al_{1+w}Si_{3-w}O_8} = w\partial\mu^{e.m.}_{CaO} + (1-w)\partial\mu^{e.m.}_{NaO_{1/2}} + (1+w)\partial\mu^{e.m.}_{AlO_{3/2}} + (3-w)\partial\mu^{e.m.}_{SiO_2}. \quad [4a]$$

Differentiating Eqn. 4a with respect to the compositional variable w, we have

$$\frac{\partial\mu^{plag}_{Ca_wNa_{1-w}Al_{1+w}Si_{3-w}O_8}}{\partial w} = \partial\mu^{e.m.}_{CaO} - \partial\mu^{e.m.}_{NaO_{1/2}} + \partial\mu^{e.m.}_{AlO_{3/2}} - \partial\mu^{e.m.}_{SiO_2}. \quad [4b]$$

This shows that an increase in the Ca/(Ca + Na) ratio of plagioclase can be accomplished by an increase in μ_{CaO} or $\mu_{AlO_{3/2}}$ or by a decrease in μ_{SiO_2} or $\mu_{NaO_{1/2}}$ in the exchange medium. These variations in μ_{CaO}, $\mu_{AlO_{3/2}}$, and μ_{SiO_2} will be established if anorthitic plagioclase, orthopyroxene, and merrillite act as a buffering assemblage.

Finally, if sufficient chromite and ilmenite were present in the corona-forming region, then these minerals could have contributed to the buffering of $\mu_{CrO_{3/2}}$ and μ_{TiO_2}. Relations [g], [i], and [j] in Table 4 suggest that variations in $\mu_{CrO_{3/2}}$ and μ_{TiO_2} should have opposed the variations in μ_{MgO} and μ_{FeO}. For most coronas in Emery, which contain orthopyroxene that is relatively uniform in Fe/Mg across coronas, both μ_{MgO} and μ_{FeO} should have increased from matrix to olivine, and thus $\mu_{CrO_{3/2}}$ and μ_{TiO_2} should have decreased from matrix toward olivine. Under these conditions $CrO_{3/2}$ and TiO_2 will tend to diffuse toward olivine. Similarly, any Cr initially present in matrix metal should have diffused toward olivine upon the breakdown of metal during corona formation, so long as a sufficient amount of chromite was present in the corona-forming region.

DISCUSSION

Timing of Corona Formation

As previously noted by POWELL (1971), coronas are formed on brecciated mineral clasts of olivine but are themselves unbrecciated, which implies that brecciation occurred before corona formation. This work supports and extends this conclusion by showing that all seventeen of the corona structures (including pseudomorphs) found in Morristown and Emery have complete and intact zone sequences, with no evidence that any of the coronas were mechanically disrupted. Similarly, DELANEY et al. (1981) noted that inverted pigeonite overgrowths on orthopyroxene clasts and orthopyroxene rims on ferrous pigeonite grains appear to have formed after brecciation. This suggests that intensive, millimeter-scale brecciation occurred before high-temperature metamorphism, although it does not rule out the possibility of postmetamorphic brecciation on a scale generally larger than that of a thin section (> few cm).

As shown in this work and by NEHRU et al. (1980), the contact between the outer zone of coronas and matrix is marked by the coincident disappearance of both tridymite and coarse matrix metal. This suggests that tridymite and coarse metal were simultaneously removed in corona-forming reactions, and that metal-silicate mixing predated corona formation. Although it is conceivable that metal was introduced after coronas had largely formed and that it did not penetrate into coronas because they were "armored" or mechanically coherent, this seems unlikely as the physical characteristics (such as grain size) of the coronas and silicate matrix are virtually identical.

Scale of Local Equilibrium

Coronas show abundant evidence for local equilibrium (see above), and the scale of local equilibrium appears to have been very small. The local equilibrium model implies that equilibrium was attained on a scale no larger than the width of smallest distinct mineral zone in the coronas, which corresponds to $\approx$100–200 μm in Emery and only $\approx$20 μm in Morristown. Departure from equilibrium is also suggested by the fairly large scatter in geothermometer temperatures (this work; NEHRU et al., 1980), and by the steep zoning profiles in some plagioclase overgrowths, which occur over less than 5 μm in both Emery and Morristown. The latter also imply that intracrystalline diffusion was especially sluggish in plagioclase compared to other phases.

Reactions

The principal corona-forming reaction was (NEHRU et al., 1980)

$$\underset{\text{olivine}}{(Mg,Fe)_2SiO_4} + \underset{\text{tridymite}}{SiO_2} \rightarrow 2\,\underset{\text{orthopyroxene}}{(Mg,Fe)SiO_3}, \qquad (1)$$

where the Fe/Mg content of orthopyroxene immediately adjacent to olivine was controlled by local equilibrium with olivine. This reaction, however, does not account for the high abundances of merrillite and chromite nor for the depletion of clinopyroxene in coronas. As discussed earlier, the likely source of P for corona merrillite is metal, suggesting that a corona-forming reaction of the following sort was important:

$$\underset{\text{clinopyroxene}}{6Ca_{0.5}Mg_{0.5}SiO_3} + \underset{\text{metal}}{2P^0} + {}^5\!/_2O_2 \rightarrow \underset{\text{merrillite}}{Ca_3(PO_4)_2} + \underset{\text{silica}}{3SiO_2} + \underset{\text{orthopyroxene}}{3MgSiO_3}. \qquad (2a)$$

If this reaction occurred at the corona-matrix contact during corona formation, it would decrease the clinopyroxene and increase the merrillite abundances in the coronas compared to matrix. A silica mineral could be produced by reaction (2a), but so long as this reaction occurred at the corona-matrix contact during corona growth, where silica minerals were locally unstable and being removed by reaction, SiO_2 would instead have been added to the diffusion medium or to other locally stable Si-rich minerals such as plagioclase. Silica added to the diffusion medium anywhere in the coronas will ultimately react with olivine to form more corona orthopyroxene via reaction (1). Although the source of Cr for corona chromite is not obvious, much of it may have originated in metal, as discussed previously. In this case, the following reaction may be written for coronas:

$$\underset{\text{metal}}{2\,Cr^0} + Fe^0 + 2\,O_2 \rightarrow \underset{\text{chromite}}{FeCr_2O_4}. \qquad (2b)$$

Alternatively, Cr may have originated in chromite or other Cr-rich minerals that were associated with matrix metal. Assuming that all SiO_2 reacts with olivine to form orthopyroxene, we may combine and simplify 2a and 2b to

olivine + clinopyroxene + P-Cr-bearing metal

$$\rightarrow \text{merrillite} + \text{orthopyroxene} + \text{Cr-spinel}. \qquad (2)$$

Coronas in Emery and Morristown differ greatly in their abundances of merrillite and chromite, and slightly in their abundance of clinopyroxene, with those in Emery being richer in merrillite and chromite and poorer in clinopyroxene (Table 1). These differences are partially explained if reaction (2) was more important in Emery than in Morristown, which is consistent with the much higher abundance of coarse matrix metal in the former meteorite. If reaction (2) proceeded to a greater extent in Emery than Morristown coronas, then the only slightly lower abundance of clinopyroxene in Emery coronas implies that removal of clinopyroxene by reaction (2) was partially offset by the production of this mineral by another reaction. One possible clinopyroxene-forming reaction is

$$\underset{\text{olivine}}{2(Mg,Fe)_2SiO_4} + \underset{\text{plagioclase}}{CaAl_2Si_2O_8} \rightarrow \underset{\text{orthopyroxene}}{2(Mg,Fe)SiO_3} + \underset{\text{clinopyroxene}}{2Ca_{0.5}(Mg,Fe)_{0.5}SiO_3} + \underset{\text{Al-spinel}}{(Mg,Fe)Al_2O_4}, \qquad (3)$$

which was originally proposed by DELANEY et al. (1981) as a way of explaining the high abundance of chromite in coronas. Depending on the relative importance of reactions (2) and (3), the composition of chromite could have become richer in Al and poorer in Cr, or vice-versa.

Some metallic Fe may also have been oxidized during corona formation, as implied by the tendency of metal blebs in coronas to be Ni-rich compared to metal in the matrix. The principal reaction may have been:

$$\underset{\text{tridymite}}{SiO_2} + \underset{\text{metal}}{Fe^0} + {}^1\!/_2O_2 \rightarrow \underset{\text{orthopyroxene}}{FeSiO_3} \qquad (4)$$

which would occur at the corona-matrix contact, where both tridymite and metal were being consumed. This oxidation of Fe is in addition to that accompanying chromite formation *via* reaction (2b). Reaction (4) may have proceeded in the opposite direction, implying reduction, in basalt/gabbro clasts in mesosiderites, based on the observation of a correlation between FeO/MnO and FeO/MgO, with later-crystallizing grains being depleted in FeO (MITTLEFEHLDT, 1990). Such a correlation, however, does not hold for corona orthopyroxene grains, which have relatively uniform FeO/MnO even when FeO/MgO varies. Evidently, the nature of redox (and possibly other) reactions varied from place to place in mesosiderites, dependent in part on local differences in the mineralogy. Different redox reactions may also have occurred at different times.

Reaction (4) could have served as the principal oxygen buffer in mesosiderites wherever a sufficient amount of tri-

dymite, orthopyroxene and metal coexisted (HARLOW et al., 1982). The net result of various equilibria between tridymite, orthopyroxene, clinopyroxene, P-bearing metal and merrillite would have been for reaction (4) to proceed to the left as temperature decreased (HARLOW et al., 1982). In this event, the reverse of reaction (4), operating in the matrix and possibly elsewhere in mesosiderites, could have been the source of oxygen that was used for oxidation in coronas.

The oxidation of Fe^0 is unlikely to have been the only cause for the drastic depletion of metal in coronas. Oxidation of a large amount of matrix metal should have resulted in a correspondingly large amount of Ni-rich metal in coronas or in nearby matrix, or in a high bulk FeO abundance for coronas, but this is not the case. There is not enough Ni-rich metal in coronas (<2 vol%) to be consistent with oxidation of large amounts of Ni-poor matrix metal (≈40 vol% in Emery). Moreover, bulk FeO contents of even chromite-rich coronas are intermediate between that of olivine and the silicate matrix. Instead, much of the Fe in matrix metal and sulfides must have diffused away from olivine during corona formation.

Nature of Metamorphism

Pyroxene geothermometry suggests that high-temperature metamorphism in mesosiderites probably involved peak temperatures of ≈950–1200°C (this work; HEWINS, 1979). The matrix of mesosiderites is rich in a eucritic basalt fraction (e.g., DELANEY et al., 1981), and eucrites have a liquidus temperature of ≈1180°C (STOLPER, 1977), which is only slightly higher than the 1000–1100°C two-pyroxene closure temperature inferred for Emery coronas. Thus, corona growth, at least in Emery, may have been initiated near the solidus while a small amount of silicate melt was present. HARLOW et al. (1982) noted that the addition of P, S, and other components, which may have been present in matrix metal initially, could have lowered the temperature of the metal solidus to below the silicate solidus. This work provides additional support for the initial presence of significant P and Cr in matrix metal, and for the possibility that the metallic fraction of mesosiderites was partially molten at the maximum temperatures experienced during metamorphism.

The relatively rapid cooling rate at high temperatures inferred for Emery and Morristown based on plagioclase overgrowths in coronas places strong constraints on the cooling environment and potential heat sources for high-temperature metamorphism. Assuming maximum heating temperatures anywhere between 950–1200°C, a cooling timescale for high-temperature metamorphism of $\approx 10^2$–10^5 years is permissible for cooling to 850°C. This cooling time scale is comparable to the heat diffusion timescale of 10^4 years for a 1 km asteroidal object (SCOTT et al., 1989), suggesting that high-temperature metamorphism of mesosiderites occurred either in a small parent body or in the near-surface environment of a larger one.

Possible heat sources for high-temperature metamorphism include decay of ^{26}Al, induction heating during a T-Tauri phase of the sun, and impact metamorphism. Heating by ^{26}Al decay appears unlikely for high-temperature mesosiderite metamorphism because the ^{26}Al heating timescale of 10^6 years (SCOTT et al., 1989) is longer than the inferred cooling time scale. Induction heating appears to be a viable heating mechanism, as the time scale of 10^4–10^7 years for induction heating (SCOTT et al., 1989) partially overlaps the inferred cooling time scale. Impact metamorphism is also a viable mechanism, especially considering the major role played by brecciation in all mesosiderites and the evidence for extensive impact melting in subgroup 4 mesosiderites. SCOTT et al. (1989) concluded that impact processes were important on asteroidal objects but that most strongly impact-heated ejecta would have been lost to space. However, mesosiderites could have formed near the basal region of one or more impact craters, where material is likely to have been both strongly heated and retained by the asteroid. RUBIN and MITTLEFEHLDT (1993) suggested localized impact melting as a likely heat source for corona formation in mesosiderites, but such heating could not have been so localized as to result in late, small-scale brecciation (see above) or in obvious metamorphic gradients on the scale of a thin section.

Mesosiderites also appear to have cooled very slowly at lower temperatures (see Introduction), possibly following a reheating episode. Some constraints can be placed on the temperature at which such slow cooling was initiated. The sharp chemical interfaces of overgrown plagioclase grains in coronas suggest that cooling rates of $\approx 10^{-6}$ °C/y must have been initiated at temperatures below 800°C. Similarly, metallographic data imply that the onset of slow cooling probably occurred above 500°C (POWELL, 1969). Thus, slow cooling was probably initiated between ≈500–800°C.

Evolution of the Mesosiderite Parent Body

RUBIN and MITTLEFEHLDT (1993) recently proposed an evolutionary history for the mesosiderite parent body (MPB) based on petrologic and chronologic constraints. This model involved the following steps.

1) Initial differentiation, metal-silicate mixing and crustal remelting prior to 4.4 Ga ago, consistent with U-Pb, Sm-Nd, or Rb-Sr internal isochrons of >4.4 Ga for most of the components in mesosiderites, including matrix metal (BROUXEL and TATSUMOTO, 1991; STEWART et al., 1991, 1992; PRINZHOFER et al., 1992).
2) Isolated impact melting 4.5–3.9 Ga ago, including the formation of impact-melted clasts, and the formation of olivine coronas and pyroxene overgrowths by the heat liberated from localized impacts.
3) Disruption of the MPB by a large impact event 3.9 Ga ago, followed by gravitational reassembly of the parent body and deep burial of the mesosiderite source region, consistent with the evidence for slow cooling (probably $\approx 10^{-6}$ °C/y) at low temperatures (<500°C) (see Introduction) and with relatively young Ar-Ar ages of 3.4–3.8 Ga (BOGARD et al., 1990).

Based on our observations of the relative timing of corona formation, it seems likely that corona formation and high-temperature metamorphism took place prior to 4.4 Ga ago, after metal-silicate mixing and after most of the small-scale brecciation had occurred. While it is conceivable that high-temperature metamorphism and corona formation occurred

later, this is considered unlikely, as heating to high temperatures would probably have significantly reset the U-Pb, Sm-Nd, and Rb-Sr systems.

The timing of the postulated large, parent-body–disrupting impact event is also unclear. Considering the uncertainties in the lower-temperature cooling rates and in Ar-Ar closure temperatures (GANGULY et al., 1994), and in the maximum temperature at which slow cooling was initiated (see above), about all that can be said with confidence is that slow cooling began prior to 3.5–3.8 Ga ago, implying the timing of the putative parent body break-up.

CONCLUSION

Olivine coronas in mesosiderites formed by a process of reaction and diffusion between olivine and mesosiderite matrix during high-temperature metamorphism. Coronas are systematically thicker in Emery than in Morristown, suggesting that the former meteorite was more intensively metamorphosed. Textural relations suggest that corona formation occurred largely after intensive small-scale brecciation and after or during metal-silicate mixing. Apparent two-pyroxene closure temperatures for coronas are ≈1000–1100°C for Emery and ≈880–930°C for Morristown. Together with pyroxene geothermometry for inverted pigeonite overgrowths (HEWINS, 1979), this suggests that high-temperature metamorphism of mesosiderites occurred over temperatures of 850–1100°C and possibly up to 1200°C. These temperatures are high enough that some silicate and metallic melt could have been present during metamorphism. Cooling rates at the peak temperature of metamorphism were rapid, ≥0.1°C/y, suggesting that high-temperature metamorphism of mesosiderites occurred near the surface of the parent body. This metamorphism may have been the result of heating by electromagnetic induction or by hypervelocity impact.

The bulk compositions of coronas, except for P and Cr, can be modelled by the reaction of ≈10–25 wt% olivine with ≈90–75 wt% metal- and sulfide-free matrix. Phosphorus and Cr appear to have been extracted from a very large volume of matrix during metamorphism, and Fe^0, Ni^0, and S largely diffused out of the corona-forming region, perhaps aided by rapid diffusion rates in metallic or silicate liquid. Prior to high-temperature metamorphism, matrix metal contained relatively high concentrations of P (≈0.6 wt%?) and possibly Cr (≈0.3 wt%?). A local equilibrium model explains many salient features of the coronas, including their mineralogical structure, the compositions of orthopyroxene and plagioclase, and evidence for the growth of plagioclase in the outer zones of coronas. In most cases $AlO_{3/2}$ appears to have diffused away from near the inner/middle zone contact in coronas toward both olivine and matrix; MgO, FeO, and CaO appear to have diffused away from olivine toward matrix; and SiO_2 and $PO_{5/2}$ appear to have diffused away from matrix toward olivine. $CrO_{3/2}$ and TiO_2 may also have diffused toward olivine from matrix. Low values of $\mu_{CrO_{3/2}}$ and $\mu_{PO_{5/2}}$ and a high value of μ_{FeO} in most coronas compared to matrix promoted the breakdown of coarse matrix metal in the coronas and enabled them to become a sink for P and Cr.

Acknowledgments—The writers wish to thank Marty Prinz for loans of the thin sections and Dave Mittlefehldt, George Harlow, Alan Rubin, Bill Carlson, George Fisher, Yukio Ikeda, and an anonymous reviewer for constructive comments that substantially improved this manuscript. This work was supported by NASA grants NAG 9-37 to W. V. Boynton and NAG 9-460 to J. Ganguly.

Editorial handling: Mittlefehldt

REFERENCES

BOGARD D. D., GARRISON D. H., JORDAN J. L., and MITTLEFEHLDT D. (1990) ^{39}Ar-^{40}Ar dating of mesosiderites: Evidence for a major parent body disruption <4 Ga ago. *Geochim. Cosmochim. Acta* **54,** 2549–2564.

BROUXEL M. and TATSUMOTO M. (1991) The Estherville mesosiderite: U-Pb, Rb-Sr, and Sm-Nd isotopic study of a polymict breccia. *Geochim. Cosmochim. Acta* **55,** 1121–1133.

BULL R. K. and DURRANI S. A. (1979) Fission track chronology of the Bondoc mesosiderite. *Meteoritics* **14,** 362–364.

BUCHWALD V. F. (1975) *Handbook of Iron Meteorites—Their History, Distribution, Composition and Structure, Vol. 1. Iron Meteorites in general.* Univ. Calif. Press.

CROZAZ G. and TASKER D. R. (1981) Thermal history of mesosiderites revisited. *Geochim. Cosmochim. Acta* **45,** 2037–2046.

CROZAZ G., ZINNER E., and DELANEY J. S. (1985) Rare earth element concentrations of mesosiderite merrillite. *Meteoritics* **20,** 629–630.

DELANEY J. S., NEHRU C. E., PRINZ M., and HARLOW G. E. (1981) Metamorphism in mesosiderites. *Proc. 12th Lunar Planet. Sci. Conf.,* 1315–1342.

DELANEY J. S., PRINZ M., and TAKEDA H. (1984) The polymict eucrites. *Proc. 15th Lunar Planet. Sci. Conf.; J. Geophys. Res.* **89,** C251–C288 (suppl.).

FLORAN R. J. (1978) Silicate petrography, classification, and origin of mesosiderites: Review and new observations. *Proc. 9th Lunar Planet. Sci. Conf.,* 1053–1081.

FLORAN R. J., CAULFIELD J. B. D., HARLOW G. E., and PRINZ M. (1978) Impact melt origin for the Simondium, Pinnaroo, and Hainholz mesosiderites: Implications for impact processes beyond the earth-moon system. *Proc. 9th Lunar Planet. Sci. Conf.,* 1083–1114.

FUCHS L. H. (1969) The phosphate mineralogy of meteorites. In *Meteorite Research* (ed. P. M. MILLMAN), pp. 683–695. Reidel.

GANGULY J., BHATTACHARYA R. N., and CHAKRABORTY S. (1988) Convolution effect in the determination of compositional profiles and diffusion coefficients by microprobe step scans. *Amer. Mineral.* **73,** 901–909.

GANGULY J., YANG H., and GHOSE S. (1994) Thermal history of mesosiderites: Constraints from compositional zoning and Fe-Mg ordering in orthopyroxenes. *Geochimica Cosmochimica Acta* **58,** 2711–2723.

GROVE T. L., BAKER M. B., and KINZLER R. J. (1984) Coupled CaAl-NaSi diffusion in plagioclase feldspar: Experiments and applications to cooling rate speedometry. *Geochim. Cosmochim. Acta* **48,** 2113–2121.

HARLOW G. E., DELANEY J. S., NEHRU C. E., and PRINZ M. (1982) Metamorphic reactions in mesosiderites: Origin of abundant phosphate and silica. *Geochim. Cosmochim. Acta* **46,** 339–348.

HEWINS R. H. (1979) The pyroxene chemistry of four mesosiderites. *Proc. 10th Lunar Planet. Sci. Conf.,* 1109–1125.

HEWINS R. H. (1984) The case for a melt matrix in plagioclase-POIK mesosiderites. *Proc. 15th Lunar Planet. Sci. Conf.; J. Geophys. Res.* **89,** C289–C297 (suppl.).

JOESTEN R. (1977) Evolution of mineral assemblage zoning in diffusion metasomatism. *Geochim. Cosmochim. Acts* **41,** 649–670.

JONES J. H. (1982) Mesosiderites: (1) Reevaluation of cooling rates and (2) experimental results bearing on the origin of metal. *Lunar Planet. Sci. XIV,* 315–352.

KORZHINSKII D. S. (1959) *Physiochemical basis of the analysis of the paragenesis of minerals.* (Translated from Russian), Consultants Bureau Inc., Chapman and Hall Ltd.

KULPECZ A. A., JR., and HEWINS R. H. (1978) Cooling rate based on schreibersite growth for the Emery mesosiderite. *Geochim. Cosmochim. Acta* **42,** 1495–1500.

LINDSLEY D. H. and ANDERSON D. J. (1983) A two-pyroxene thermometer. *Proc. 13th Lunar Planet. Sci. Conf.,* A887–A906.

MEDARIS L. G., JR. (1969) Partitioning of Fe^{++} and Mg^{++} between

coexisting synthetic olivine and orthopyroxene. *Amer. J. Sci.* **267,** 945–968.

MITTLEFEHLDT D. W. (1990) Petrogenesis of mesosiderites: I. Origin of mafic lithologies and comparison with basaltic achondrites. *Geochim. Cosmochim. Acta* **54,** 1165–1173.

NEHRU C. E., S. M. ZUCKER, HARLOW G. E., and PRINZ M. (1980) Olivines and olivine coronas in mesosiderites. *Geochim. Cosmochim. Acta* **44,** 1103–1118.

PERRON C., BOUROT-DENISE M., and MOSTEFAOUI S. (1992) Bishunpur and Semarkona: New clues to the origin of inclusions in metal. *Meteoritics* **27,** 275–276.

POWELL B. N. (1969) Petrology and chemistry of Mesosiderites—I. Textures and composition of nickel-iron. *Geochim. Cosmochim. Acta* **33,** 789–810.

POWELL B. N. (1971) Petrology and chemistry of mesosiderites—II. Silicate textures and compositions and metal-silicate relationships. *Geochim. Cosmochim. Acta* **35,** 5–34.

PRINZ M., NEHRU C. E., DELANEY J. S., HARLOW G. E., and BEDELL R. L. (1980) Modal studies of mesosiderites and related achondrites, including the new mesosiderite ALHA 77219. *Proc. 11th Lunar Planet. Sci. Conf.*, 1055–1071.

PRINZHOFER A., PAPANASTASSIOU D. A., and WASSERBURG G. J. (1992) Samarium-neodymium evolution of meteorites. *Geochim. Cosmochim. Acta* **56,** 797–815.

RAMBALDI E. R. and WASSON J. T. (1984) Metal and associated phases in Krymka and Chainpur: Nebular formational processes. *Geochim. Cosmochim. Acta* **48,** 1885–1895.

RUBIN A. E. and MITTLEFEHLDT D. W. (1993) Evolutionary history of the mesosiderite asteroid: A chronologic and petrologic synthesis. *Icarus* **101,** 201–212.

SCOTT E. R. D., TAYLOR G. J., NEWSOM H. E., HERBERT F., ZOLENSKY M., and KERRIDGE J. F. (1989) Chemical, thermal and impact processing of asteroids. In *Asteroids II* (ed. R. P. BINZEL et al.), pp. 701–739. Univ. Arizona Press.

STEWART B. W., CHENG Q. C., PAPANASTASSIOU D. A., and WASSERBURG G. J. (1991) Sm-Nd systematics of mesosiderites. *Lunar Planet. Sci. XXII,* 1333–1334.

STEWART B. W., PAPANASTASSIOU D. A., and WASSERBURG G. J. (1992) Sm-Nd chronology and petrochemistry of mesosiderites. *Lunar Planet. Sci. XXIII,* 1356–1366.

STOLPER E. (1977) Experimental petrology of eucritic meteorites. *Geochim. Cosmochim. Acta* **41,** 587–611.